Phase Cancellation in Backscatter-Based Tag-to-Tag Communication Systems

Zhe Shen, Akshay Athalye and Petar M. Djurić

***Abstract*—In this paper, we investigate a unique phase cancellation problem that occurs in backscatter-based tag-to-tag (BBTT) communication systems. These are systems wherein two or more radio-less devices (tags) communicate with each other purely by reflecting (backscattering) an external signal (whether ambient or intentionally generated). A transmitting tag modulates baseband information onto the reflected signal using backscatter modulation. At the receiving tag, the backscattered signal is superimposed to the external excitation and the resulting signal is demodulated using envelope detection techniques. The relative phase difference between the backscatter signal and the external excitation signal at the receiving tag has a large impact on the envelope of the resulting signal. This often causes a complete cancellation of the baseband information contained in the envelope, and it results in a loss of communication between the two tags. This problem is ubiquitous in all BBTT systems and greatly impacts the reliability, robustness, and communication range of such systems. We theoretically analyze and experimentally demonstrate this problem for devices that use both ASK and PSK backscattering. We then present a solution to the problem based on the design of a new backscatter modulator for tags that enables multi-phase backscattering. We also propose a new combination method that can further enhance the detection performance of BBTT systems. We examine the performance of the proposed techniques through theoretical analysis, computer simulations, and lab experiments with a prototype tag that we have developed.**

***Index Terms*—Radio-frequency identification (RFID), phase cancellation, multi-phase backscatter**

I. Introduction

The science behind communication by means of reflected signals or backscatter has been studied for several decades. In recent years this technique has seen widespread practical application in the form of Radio Frequency Identification (RFID). Furthermore, it is expected that the RFID technology will play a prominent role in enabling the Internet of Things (IoT), where physical objects will be connected to other objects and to the cyberspace. Typical backscatter RFID systems consist of an active reader that transmits a query signal and passive tags that communicate with the reader by reflecting part of this signal. This communication technique allows for tags that are very inexpensive and consume very low power.

Traditional passive RFID has long been thought of as the 'last link' in the IoT, enabling visibility and connectivity for all items regardless of size, cost and volume [1]. This is primarily due to the very low cost and low power consumption of passive RFID tags. However, use of traditional RFID technology requires a centralized model wherein one high-cost reader initiates and controls communication with a population of tags in its vicinity. The reader-tag links are between 3 m to 6 m depending upon the type of tag, the size of reader antenna and application environment. Thus, the covering of a large area with a reader-based RFID system requires the deployment of multiple readers. In these systems, the readers send out a high strength modulated query signal to a population of tags. As a result, reader-to-reader interference becomes a significant issue [2]. This further complicates the deployment procedure. Moreover, the readers themselves need to be part of a network so that the query procedures can be coordinated and tag data from each reader can be aggregated. All these factors make large scale RFID deployments very costly which is a difficult barrier to entry for ubiquitous RFID deployment.

Backscatter based tag-to-tag communication (BBTT) is a paradigm that can overcome the above limitations and help realize the vision of the IoT. It can allow ubiquitously tagged objects to independently communicate with each other without being controlled by a single reader. In these systems, passive radio-less tags communicate by reflecting an external excitation signal. The external exciter does not need to send out modulated commands or decode tag responses. This makes the exciters required for a BBTT deployment an order of magnitude lower in cost than RFID readers. Moreover, the exciters do not need to be networked or synchronized in any way. This minimizes the deployment effort. In many cases, BBTT deployments can make use of pre-existing sources of excitation in an application environment such as TV towers [3] and wireless access points [4]. In these cases, the deployment cost and effort for the BBTT system would be almost zero.

Conventional reader-tag systems have already found widespread applications. However, the scale and ubiquity of these systems is limited for reasons discussed above. With its unprecedented scalability advantages and low cost, the BBTT paradigm allows such systems to be deployed at a much larger scale and at much reduced cost. The applications range from scenarios where only two tags communicate with each other (e.g., credit card payments, access control) to cases where a large number of tags communicate using multi-hop backscatter communication (e.g., inventory control, environment monitoring, warehouse management). In addition, the ability of tags to communicate directly and autonomously with each other opens up a whole new set of practical use cases. An important class of such applications is proximity detection. In these applications, the goal is to detect interactions between different objects and their relative proximity to one another without needing to know their absolute locations. This will enable detection of interactions between objects and people, one of the core visions of the future IoT [5], [6]. Beneficiaries of all these advancements will include the healthcare service industry, food-supply chains, homes for assisted living, the pharmaceutical industry, security, and retail.

The passive tag-to-tag communication has recently started to gain research interest. Communication between two passive RFID tags at close range using backscatter communication has been demonstrated in [7] and the electromagnetic models that govern the communication in this system have been explored in [8]. In our previous work, we have developed a radio-less EPC Gen 2 compliant device (the sensatag) that can listen to backscatter signals from neighboring Gen 2 RFID tags and in turn communicate with a Gen 2 RFID reader using standard backscatter modulation [9]. We employed this device to enable precise localization and tracking in passive RFID systems

Z. Shen was with the Department of Electrical and Computer Engineering, Stony Brook University, Stony Brook, NY 11794, USA, and is now with Google, Mountain View, CA 94043, USA. A. Athalye is with Scandent, LLC, NY, USA and the Department of Electrical and Computer Engineering, Stony Brook University, Stony Brook, NY 11794, USA. P. M. Djurić is with the Department of Electrical and Computer Engineering, Stony Brook University, Stony Brook, NY 11794, USA.

Emails: zhe.shen, akshay.athalye, petar.djuric@stonybrook.edu.

This work was supported by NSF under Awards CNS-1405740 and ECCS-1346854.

[10].

All these systems employ a standard UHF RFID reader as the source of the excitation signal to enable the backscatter communication. In [3], the authors have designed a system where tags communicate by backscattering ambient TV signals. Similarly, in [4] a backscatter-based communication system that uses ambient WiFi signals as excitation source has been demonstrated. Although the frequency of the excitation signal and the sources of power for the tag differ in the above systems, the general design of the tags is similar. The tags consist of an antenna, a backscatter modulator, an envelope detection circuit, a comparator for digitizing the detected envelope, and a digital controller that implements the chosen communication protocol. The backscatter modulator consists of a switch that alters the reflection cross section (RCS) of the antenna between two states by varying the termination impedance. This allows for modulation of baseband data onto the reflected backscatter signal. Tags can employ ASK or PSK backscatters. In the former case, the real part, and in the latter, the imaginary part of the RCS are varied, respectively.

In this paper, we explore phase cancellation issues that occur in such BBTT communication systems. Consider two tags in a BBTT scenario, both receiving an excitation signal, either from an active source or ambient radiation. The transmitting tag sends out baseband data using backscatter modulation. The receiving tag sees a signal that is a superposition of the excitation signal and the modulated backscatter from the transmitting tag. Since the tags are passive radio-less devices, the receiving tag cannot implement active IQ demodulation to extract the backscatter signal. Instead, it has to rely on passive envelope demodulation. In such a setup, the relative phase difference between the excitation signal and the modulated backscatter at the receiving tag has a big impact on the amplitude of the baseband envelope in the combined signal.

Based on the value of the phase difference between the excitation and backscatter signals, the baseband envelope can be severely attenuated and completely cancelled out leading to a loss of communication between the two tags. Due to this phase problem, the amplitude of the received baseband signal does not decrease monotonically with increasing distance between the two tags. Instead, it varies between peaks and nulls, with the peaks getting successively smaller. This phenomenon significantly impairs the robustness of the tag-to-tag link.

In order to truly unlock the potential of BBTT communication, it is important that the tags can communicate over long distances with low bit error rates (BERs). Handling the challenge of phase cancellation is a critical step towards achieving that goal. We present a mathematical formulation of the phase problem and further illustrate it using phasor diagrams. We verify the models using simulations and lab experiments with a prototype tag that we have designed. In order to solve this problem, we propose a new backscatter modulation technique that uses phase diversity. We couple it with a combination scheme in the tag front end that can further exploit this diversity and increase the link range and robustness.

In summary, backscattering devices are traditionally intended to communicate with an active reader. Hence over the past decade much of the design and optimization efforts have gone towards building devices to achieve this goal. The BBTT paradigm, on the other hand, opens up a new set of challenges which call for novel designs of backscatter modulators and tag front end circuits. Our solutions from this paper are one response to some of these challenges.

The rest of the paper is organized as follows. In Section II we explain the phase cancellation problem in BBTT systems. There we provide a mathematical formulation of it along with phasor diagrams for systems utilizing both ASK and PSK backscattering. Then in Section III we first describe some possible solutions and in Section IV we present a solution using phase-diverse backscatter modulation. In Section V we demonstrate the phase problem and our solutions. To that end, we use MATLAB simulations. In Section VI we provide experimental results performed with a prototype tag which we have developed. The experiments confirm the simulation results. Section VII concludes the paper.

II. The Phase Cancellation Problem

Passive tags achieve backscatter modulation by varying the complex impedance of the tag chip between two or more states. This alters the complex power reflection coefficient, s^2, and accordingly alters the amplitude and/or the phase of the reflected signal. The coefficient s^2 determines what fraction of the power incident on the tag is reflected. It can be expressed as [11], [12]

$$|s|^2 = \left|\frac{Z_C - Z_A^*}{Z_C + Z_A^*}\right|^2, 0 \leq |s|^2 \leq 1, \quad (1)$$

where Z_C and Z_A are the impedances of the tag chip and tag antenna, respectively.

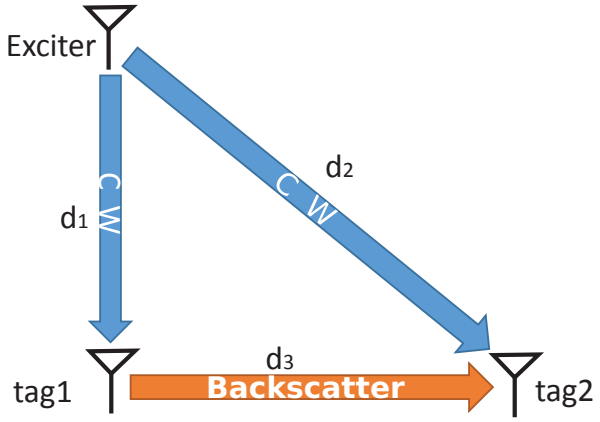

Fig. 1. A two-tag BBTT system. The respective distances between the devices are d_1, d_2, and d_3.

In Fig. 1, for simplicity, we depict a BBTT system with one exciter and only two tags. The exciter broadcasts the CW signal, and Tag 1 backscatters this signal and modulates the backscatter by varying its impedance between two states, $'0'$ and $'1'$. Tags can employ either ASK or PSK backscattering. In ASK backscattering, the real part of the chip impedance is varied between the two states by altering the amplitude of the reflected signal. By contrast, in PSK backscattering the imaginary part of the chip impedance is varied by changing the phase of the reflected signal.

The signal power received by Tags 1 and 2 from the exciter is given by Friis' equations, i.e.,

$$P_{E\to T_1} = \frac{P_E G_E G_{T_1} \lambda^2}{(4\pi d_1)^2}, \quad (2)$$

$$P_{E\to T_2} = \frac{P_E G_E G_{T_2} \lambda^2}{(4\pi d_2)^2}, \quad (3)$$

where P_E is the output power of the exciter; G_E, G_{T_1} and G_{T_2} are the antenna gains of the exciter, Tag 1 and Tag 2, respectively; $\lambda = \frac{c}{f}$ is the wavelength of the signal; f is the frequency of the signal; c is the speed of light in free space; and d_1 and d_2 are distances as shown in Fig. 1.

When tag T_1 is backscattering, its reflected power corresponding to the two backscatter modulation states can be written as

$$P_{T_1}^0 = k_0^2 P_{E\to T_1}, \quad (4)$$

$$P_{T_1}^1 = k_1^2 P_{E\to T_1}, \quad (5)$$

where k_0^2 and k_1^2 are constants proportional to the reflection coefficient of the tag, $|s|^2$, in each of the two states. Again, using Friis' equation, the power received at tag T_2 from tag T_1 in the two states can be written as

$$\begin{aligned} P^0_{T_1\to T_2} &= \frac{P^0_{T_1} G_{T1} G_{T2} \lambda^2}{(4\pi d_3)^2} \\ &= \frac{k_0^2 P_E G_E G^2_{T1} G_{T_2} \lambda^4}{(4\pi d_1)^2 (4\pi d_3)^2}, \end{aligned} \tag{6}$$

$$\begin{aligned} P^1_{T1\to T2} &= \frac{P^1_{T_1} G_{T1} G_{T2} \lambda^2}{(4\pi d_3)^2} \\ &= \frac{k_1^2 P_E G_E G^2_{T1} G_{T2} \lambda^4}{(4\pi d_1)^2 (4\pi d_3)^2}. \end{aligned} \tag{7}$$

We note that in the case of PSK these two powers are the same.

Tag 2 "sees" the superposition of two signals, viz., the CW from the exciter and the modulated backscatter from Tag 1. Since tag T_2 is a passive device, it employs an envelope detector to decode the backscatter signal received from tag T_1. Depending upon the relative phase difference between the received exciter and backscatter signals at tag T_2, the amplitude of the resultant signal may be the same in both states $'0'$ and $'1'$. When this occurs, the envelope detector is unable to detect the modulated backscatter despite tag T_1 being in the *range* of tag T_2 w.r.t. signal strength. This creates a "null spot" where the two tags cannot communicate. This phenomenon, which we refer to as phase cancellation, occurs with both ASK and PSK backscattering. We analyze the ASK and PSK modulations next.

A. ASK modulation

When the system uses ASK backscatter modulation, the tag alters the amplitude of the reflected signal in the states $'0'$ and $'1'$. The phase of the reflected signal in the two states remains the same. Let $S^0(t)$ and $S^1(t)$ represent the resultant superimposed signals received at tag T_2 when backscattering tag T_1 is in state $'0'$ and $'1'$, respectively. Furthermore, let $A^0_{T_1}$ and $A^1_{T_1}$ be the amplitudes of the received backscatter signal from tag T_1 in the two states, and let θ_E and θ_{T1} be the phases of the signals from the exciter and T_1 "seen" by T_2, respectively (the exciter is at phase 0). We point out that since this is ASK backscattering, θ_{T1} will be the same in states $'0'$ and $'1'$.

From the geometry shown in Fig. 1, we can write the following expressions for the above mentioned phases:

$$\theta_E = \frac{2\pi f d_2}{c}, \tag{8}$$

$$\theta_{T_1} = \theta_{E\to T_1} + \theta_b + \frac{2\pi f d_3}{c}, \tag{9}$$

where $\theta_{E\to T_1}$ is the phase difference of the CW signal from the exciter at T_1, and θ_b is the phase difference introduced by the backscattering hardware. Using (8) and (9), the relative phase difference, θ_d, between the two superimposing signals at T_2 is given by:

$$\begin{aligned} \theta_d &= \theta_{T1} - \theta_E \\ &= \frac{2\pi f(d_1 + d_3 - d_2)}{c} + \theta_b. \end{aligned} \tag{10}$$

Then we can write

$$\begin{aligned} S^1(t) &= A_E \cos(\omega t + \theta_E) + A^1_{T_1} \cos(\omega t + \theta_{T_1}) \\ &= A_E \cos\omega t \cos\theta_E - A_E \sin\omega t \sin\theta_E \\ &\quad + A^1_{T_1} \cos\omega t \cos\theta_{T_1} - A^1_{T_1} \sin\omega t \sin\theta_{T_1} \\ &= (A_E \cos\theta_E + A^1_{T_1} \cos\theta_{T_1}) \cos\omega t \\ &\quad - (A_E \sin\theta_E + A^1_{T_1} \sin\theta_{T_1}) \sin(\omega t). \end{aligned} \tag{11}$$

The expression for $S^0(t)$ is analogous. Let A^0 and A^1 represent the amplitudes of the signal detected by the evelope detector of T_2 in the two states. Then we have

$$\begin{aligned} &A^1 = \\ &\sqrt{(A_E \cos\theta_E + A^1_{T_1} \cos\theta_{T_1})^2 + (A_E \sin\theta_E + A^1_{T_1} \sin\theta_{T_1})^2} \\ &= \sqrt{A_E^2 + 2A_E A^1_{T_1} \cos\theta_d + (A^1_{T_1})^2}, \end{aligned} \tag{12}$$

and

$$\begin{aligned} &A^0 = \\ &\sqrt{(A_E \cos\theta_E + A^0_{T_1} \cos\theta_{T_1})^2 + (A_E \sin\theta_E + A^0_{T_1} \sin\theta_{T_1})^2} \\ &= \sqrt{A_E^2 + 2A_E A^0_{T_1} \cos\theta_d + (A^0_{T_1})^2}. \end{aligned} \tag{13}$$

Phase cancellation arises when the above two amplitudes are equal, i.e., when $A^0 = A^1$. This entails that in that case tag T_2 cannot detect and demodulate the signal sent from tag T_1. From the above equations we can determine that phase cancellation takes place when

$$\begin{aligned} &\sqrt{A_E^2 + 2A_E A^0_{T_1} \cos\theta_d + (A^0_{T_1})^2} \\ &\qquad = \sqrt{A_E^2 + 2A_E A^1_{T_1} \cos\theta_d + (A^1_{T_1})^2}, \end{aligned}$$

or when

$$\theta_d = \theta_c = \cos^{-1}\left(-\frac{A^0_{T_1} + A^1_{T_1}}{2A_E}\right), \tag{14}$$

where θ_c represents the angle at which phase cancellation occurs.

Using the power - amplitude relationship $P = A^2/2R$ where R is the input resistance of the detector circuit, we get the following relations for amplitudes of signals received at T_2

$$\begin{aligned} A_E &= A_{E\to T_2} = \sqrt{2P_{E\to T_2} R_{T_2}} \\ &= \frac{\lambda\sqrt{2P_E G_E G_{T_2} R_{T_2}}}{4\pi d_2}, \end{aligned} \tag{15}$$

$$\begin{aligned} A^0_{T_1} &= A^0_{T_1\to T_2} = \sqrt{2P^0_{T_1\to T_2} R_{T_2}} \\ &= \frac{k_0 G_{T_1} \lambda^2 \sqrt{2P_E R_{T_2} G_E G_{T_2}}}{16\pi^2 d_1 d_3}, \end{aligned} \tag{16}$$

$$\begin{aligned} A^1_{T_1} &= A^1_{T_1\to T_2} = \sqrt{2P^1_{T_1\to T_2} R_{T_2}} \\ &= \frac{k_1 G_{T_1} \lambda^2 \sqrt{2P_E R_{T_2} G_E G_{T_2}}}{16\pi^2 d_1 d_3}. \end{aligned} \tag{17}$$

Substituting from (15) into (14), we conclude that cancellation takes place when $\theta_d = \theta_c$, where

$$\theta_c = \cos^{-1}\left(-\frac{(k_0 + k_1) d_2 \lambda G_{T1}}{8\pi d_1 d_3}\right). \tag{18}$$

The phase cancellation phenomenon is shown in Fig. 2. The blue line (marker x) represents the signal received from the exciter at T_2 ($E \to T_2$), and the green line (marker $\triangle$) shows the signal received at T_2 from T_1 in states $'0'$ and $'1'$ ($T_1 \to T_2$). The superimposed signals S_0 and S_1 are plotted in purple (marker o), and the envelope, with amplitudes A^0 and A^1 is shown in red. When $\theta_d \neq \theta_c$, we can see that $A^0 \neq A^1$. Hence the envelope detector will be able to differentiate between the two levels and demodulate the backscatter signal allowing for communication between T_1 and T_2. However, as seen in Fig. 2, when $\theta_d = \theta_c$, then the amplitude of the received envelope in the two states is the same, i.e., $A^0 = A^1$. In this case the envelope detector will be unable to demodulate the tag backscatter leading to a loss of communication between the two tags.

The phase cancellation phenomenon is further illustrated in Figs. 3 and 4 with phasor diagrams showing the signals received at T_2 with and without phase cancellation, respectively. The resultant envelope

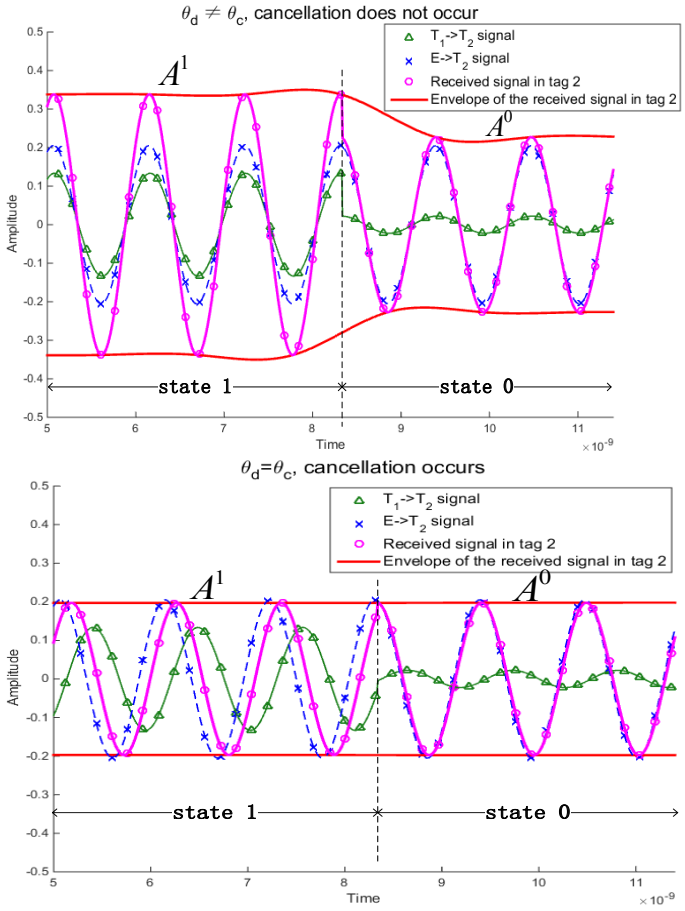

Fig. 2. Top: Signal waveforms when there is no phase cancellation ($\theta_d \neq \theta_c$). Bottom: Signal waveforms when phase cancellation takes place ($\theta_d = \theta_c$).

amplitudes A^0 and A^1 received at T_2 in the two states are obtained by adding the vectors representing the signals received from the exciter and from the backscattering tag T_1 in the two states.

B. PSK modulation

When the system uses PSK backscatter modulation, the tag T_1 changes only the phase of the reflected signal in the states $'0'$ and $'1'$. The amplitude of the reflected signal in the two states is the same. At the receiving tag, this PSK backscatter signal superimposes with the CW signal from the exciter to produce two resultant signals, one for each state $'0'$ and $'1'$. As before, if the amplitudes of the resultant signals in the two states are equal, then the envelope detector will not be able to demodulate the backscatter signal. In this subsection, we analyze the phase cancellation phenomenon in a BBTT system utilizing PSK backscattering.

In PSK modulation, the amplitudes of the two states $'0'$ and $'1'$ are the same, i.e., $A^0_{T_1} = A^1_{T_1} = A_{T_1}$. Using (15), we can write

$$A_E = A_{E\to T_2} = \frac{\lambda\sqrt{2P_E G_E G_{T_2} R_{T_2}}}{4\pi d_2}, \quad (19)$$

$$A_{T_1} = A_{T_1\to T_2} = \frac{kG_{T_1}\lambda^2\sqrt{2P_E R_{T_2} G_E G_{T_2}}}{16\pi^2 d_1 d_3}, \quad (20)$$

where k is a constant determined by the cross-section of the antenna of Tag 1.

The tag backscatters PSK signals by varying the imaginary (reactance) part of its power reflection coefficient between the two states. Let $\psi \in (0, 2\pi)$ be the phase difference between the signals

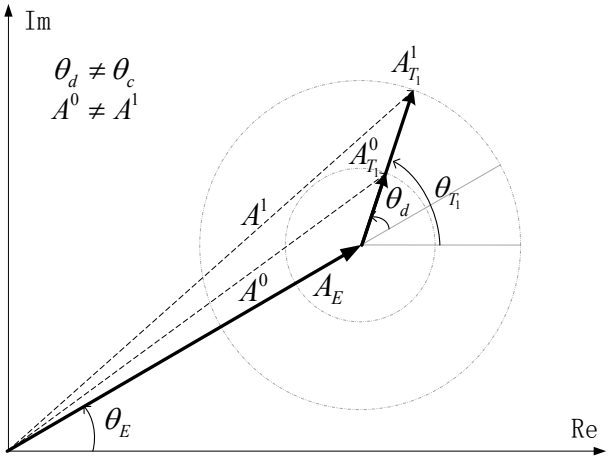

Fig. 3. A phasor diagram of ASK modulation when phase cancellation does not occur. All the symbols are defined in the text.

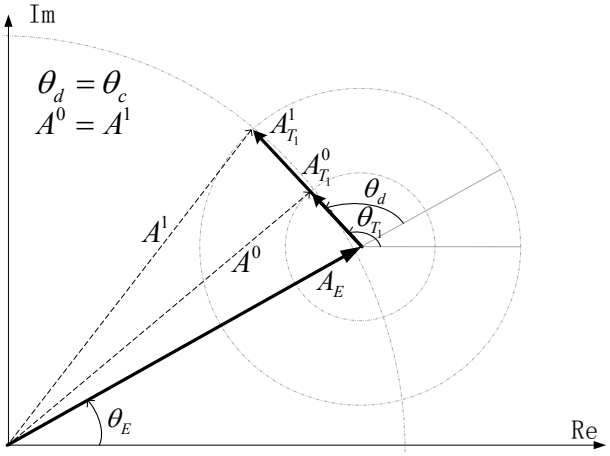

Fig. 4. A phasor diagram of ASK modulation that represents settings with phase cancellation. All the symbols are defined in the text. Note that there are two angles θ_c of phase cancellation.

backscattered in states $'0'$ and $'1'$. For the phases of the states, we can write

$$\theta^0_{T_1} = \theta^0_{T_1\to T_2} = \frac{2\pi f(d_1+d_3)}{c} + \theta_b, \quad (21)$$

$$\theta^1_{T_1} = \theta^1_{T_1\to T_2} = \theta^0_{T_1} + \psi = \frac{2\pi f(d_1+d_3)}{c} + \theta_b + \psi, \quad (22)$$

where θ_b is the phase difference introduced by the backscattering mechanism of state $'0'$, and $\theta_b + \psi$ is the phase difference due to state $'1'$.

Similarly to the ASK modulation case, the resultant signals received at T_2 when T_1 utilizes PSK backscattering can be written as

$$S^0_{PSK}(t) = A_E\cos(\omega t + \theta_E) + A_{T_1}\cos(\omega t + \theta^0_{T_1}), \quad (23)$$

$$S^1_{PSK}(t) = A_E\cos(\omega t + \theta_E) + A_{T_1}\cos(\omega t + \theta^0_{T_1} + \psi). \quad (24)$$

We can write the phase differences between the two superimposing signals, viz., the exciter signal and backscatter from T_1 at T_2 in the two states as:

$$\theta^0_d = \theta^0_{T_1} - \theta_E = \frac{2\pi f(d_1+d_3-d_2)}{c} + \theta_b, \quad (25)$$

$$\theta^1_d = \theta^1_{T_1} - \theta_E = \theta^0_d + \psi = \frac{2\pi f(d_1+d_3-d_2)}{c} + \theta_b + \psi. \quad (26)$$

Substituting from (25), (26) into (23), (24) and solving, we get the resultant envelope amplitudes in the two states as

$$A^0 = \sqrt{A_E^2 + 2A_E A_{T_1} \cos\theta_d^0 + (A_{T_1})^2}, \quad (27)$$

$$A^1 = \sqrt{A_E^2 + 2A_E A_{T_1} \cos\theta_d^1 + (A_{T_1})^2} = \sqrt{A_E^2 + 2A_E A_{T_1} \cos(\theta_d^0 + \psi) + (A_{T_1})^2}. \quad (28)$$

As explained earlier, phase cancellation occurs when $A^0 = A^1$. Then, from (27) and (28) we deduce that this happens when $\cos\theta_d^0 = \cos(\theta_d^0 + \psi)$. Thus, the condition for phase cancellation is

$$\theta_d^0 = \theta_c = n\pi - \frac{\psi}{2}, n = 0, 1, 2, \ldots \quad (29)$$

Figures 5 and 6 show the phasor diagrams of signals received at T_2 when T_1 is backscattering using PSK modulation. The phasor diagrams depict the conditions where phase cancellation does not occur and where it occurs. We can see that the signals of the two states have equal amplitudes. However, the different phases of the states cause that the received signals have different amplitudes A^0 and A^1, unless there is phase cancellation.

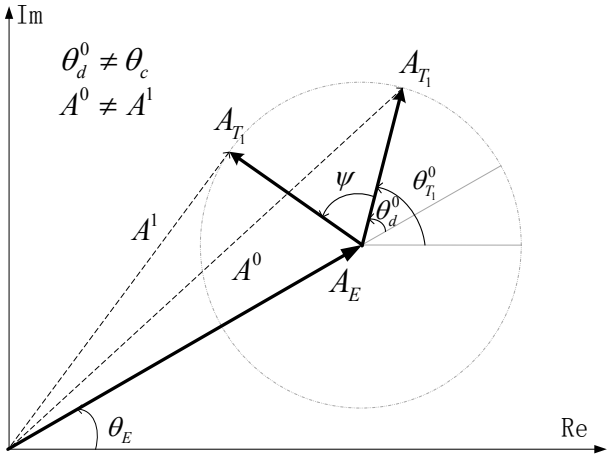

Fig. 5. A phasor diagram of PSK modulation when there is no phase cancellation. All the symbols are defined in the text.

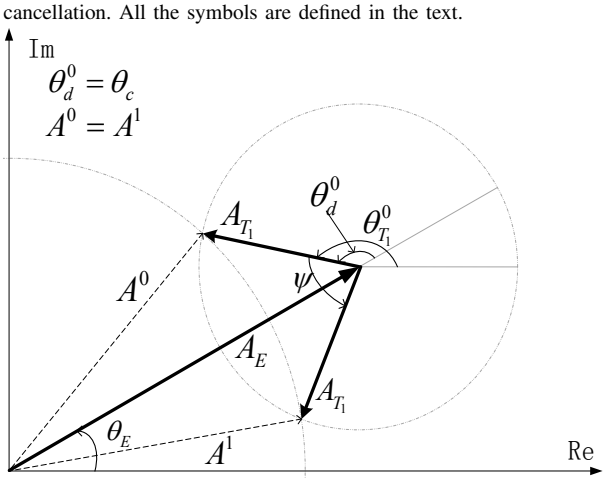

Fig. 6. A phasor diagram of PSK modulation that represents settings with phase cancellation. All the symbols are defined in the text. Note that there are two angles θ_c of phase cancellation.

III. Possible Solutions

One solution for the phase cancellation problem is a tag design with multiple antennas [13], [14]. In [13], a design for ASK modulation with a dual-antenna is addressed. If the two received signals by the antennas have different phases θ_d, the phase cancellation can be avoided in some cases. For the PSK modulation, we can also use multiple antennas. The solution based on multiple antennas may be of limited value if the distance between the two antennas is small. In that case, the difference between A^0 and A^1 may be below the detecting threshold of the envelope detector.

Another solution can be based on sending the same message two or more times (time multiplex) or use frequency hopping by the exciters. According to the time multiplex, during one transmission, the tag sends a message in the usual way, and in other time slots, the tag resends the message but with different parameters that affect θ_b and ψ in (25) and (26). In that case, at least one transmission will satisfy $\theta_d \neq \theta_c$. We note that in our system, the positions of the exciter and the tags are fixed, and therefore we can only change θ_b, f, k_0 and k_1. The frequency can only be changed by the exciters and therefore, this solution is only possible when the exciters can be controlled. For example, one may have two or more synchronized exciters that emit CWs at different frequencies. Another possibility is to have the exciters employ frequency hopping. The effectiveness of this solution would depend on the bandwidth of the frequency hopping. For UHF RFID signals, this solutions would provide poor results.

In the next section we present our proposed solution based on changing θ_b.

IV. Solutions based on phase-diverse backscatter modulation

Our proposed solution is based on the introduction of phase diversity in the backscattering via the use of an enhanced backscatter modulator. Unlike the multiple antenna approach, this solution keeps the size of the tag small. Moreover, the phase diversity introduced by a multiple antenna solution is non-deterministic and depends upon the separation between the antennas and the random geometries created by the environment. In order to achieve sufficient phase diversity, the separation between the antennas may need to be large which further increases tag size. By using an enhanced backscatter modulator, we can introduce a deterministic phase diversity into the backscatter link irrespective of the environment. This will allow systems to overcome the phase cancellation problem without requiring multiple antennas. Our proposed solution uses multi-phase backscattering employed by the transmitting tag. The tag will backscatter its information in two successive intervals with a deterministic phase difference between the backscattered signal in the two intervals. The use of phase diversity in backscattering implies that if there is a cancellation during one of the intervals, it is avoided in the other. In a straightforward implementation, this scheme will increase the robustness of the tag-to-tag link while reducing the throughput. However, in our future work, we will explore higher layer protocol mechanisms which introduce a handshaking mechanism to first determine the optimal phase to use in backscattering and then transmitting the information only once.

We now describe the proposed solution for the case of ASK modulation and PSK modulation.

A. ASK modulation with multi-phase backscattering

Under this scheme, a backscattering tag will send out its data in two successive intervals. In each of these two intervals the tag uses different phases θ_b, which according to (10) creates two different phase differences between the excitation signal and backscatter signal at the receiving tag. A standard implementation of ASK modulation requires the use of two different impedances of the tag. By contrast, in the proposed solution, we use four impedances. Our design,

shown in Fig. 7 (see also [9]), is similar to the QAM (Quadrature Amplitude Modulated) backscatter scheme from [15], [16], and [17]. The symbols Z_1 and Z_2 are two impedances with different real parts and the same imaginary part of the states $'0'$ or $'1'$, respectively. On the other hand, the impedances Z_3 and Z_4 are chosen such that the backscatter signals have the same amplitudes as when Z_1 or Z_2 are used, but their imaginary part is different from that of Z_1 and Z_2, respectively. As a result, the phase of the backscatter signals when they are used is changed.

Without loss of generality, we consider the phase of the backscatter signals to be 0 when Z_1 or Z_2 are used and θ_n when Z_3 or Z_4 are selected.

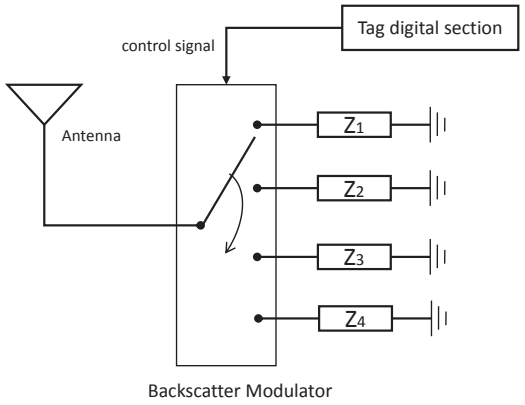

Fig. 7. Block diagram of the new tag that uses four impedances for the ASK modulation.

As described earlier, in the first interval, the backscatter modulator switches the tag impedance between Z_1 and Z_2. In the next interval, this tag sends the same message again by switching between Z_3 and Z_4. In (18), the argument of arccos is $\frac{-(k_1+k_0)d_2\lambda G_{T1}}{8\pi d_1 d_3} < 0$, so the first θ_c is in the range of $(\frac{\pi}{2}, \pi]$, and for the second one we have $(2\pi - \theta_c) \in [\pi, \frac{3\pi}{2})$. The range of θ_d can be $[0, 2\pi)$, so phase cancellation can occur at two values of θ_d in one period.

The envelope detector has a threshold for discriminating the state $'0'$ from state $'1'$, and therefore our objective is to maximize $|A^1 - A^0|$. From Fig. 3, when $\theta_d = 0$ or π, we obtain the optimum result, which is $|A^1 - A^0| = |A^1_{T1} - A^0_{T1}|$. Therefore the optimum solution is to make $\theta_n = \pi - \theta_d$ or $2\pi - \theta_d$ ($\theta_n \geq 0$). But this solution requires a tag with increased hardware complexity, which goes against the reason why we use the backscatter-based system. So we use a fixed value of θ_n.

Because we only focus on θ_d, without loss of generality, we assume $\theta_E = 0$. In Fig. 8, when $\theta_d = \theta_c$, the phase cancellation occurs during the first period. During the second period, θ_d is increased by θ_n, and then $A^0 \neq A^1$, which entails that phase cancellation does not occur. The phase θ_n is determined by Z_3 and Z_4. When considering the implementation of the proposed backscatter modulator, the values of the impedances to generate a specified phase difference in the backscattered signal can be calculated using methods described in [15] and [16].

B. PSK modulation with multi-phase backscattering

Our proposed method can also be used for PSK modulation. The implementation is similar in that it uses a backscatter modulator with four impedances and the tag sends the same message in two successive intervals. In the case of PSK modulation, the real parts of all impedances $Z_1 \cdots Z_4$ are the same and the difference between the imaginary parts of Z_1 and Z_2 is the same as that between those of Z_3 and Z_4. This means that the PSK modulation index is the same in the two intervals, but there is deterministic phase difference between the signals received in the two intervals. We note that the performance for PSK modulation is better than that for ASK modulation. The reason is that the phase cancellation can theoretically be fully avoided when the phase difference between the two pair of impedances θ_n is in $(0, \frac{\pi}{2}]$. When phase cancellation occurs, the phase differences of the two states θ^0_d and $\theta^1_d = \theta^0_d + \psi$ are symmetrical about the $n\pi$-axis. So when they both add $\theta_n \in (0, \frac{\pi}{2}]$, they will not be symmetrical anymore. A phasor diagram representing this is shown in Fig. 9. There is phase cancellation in the first period and so $\theta^0_d = \theta_c$ and $A^0 = A^1$. Then in the second period, the phases of the two states are changed by θ_n and for the amplitudes we have $A'_0 \neq A'_1$.

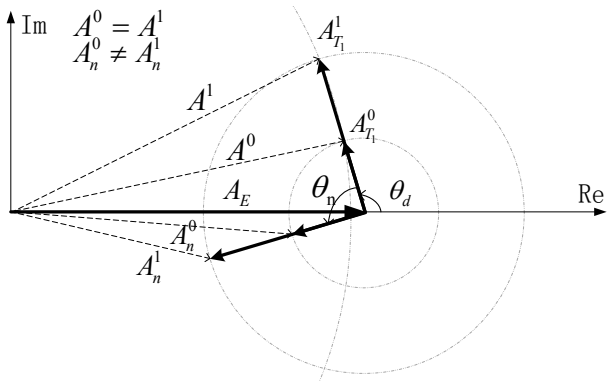

Fig. 8. Phasor diagrams of multi-phase backscattering and ASK modulation.

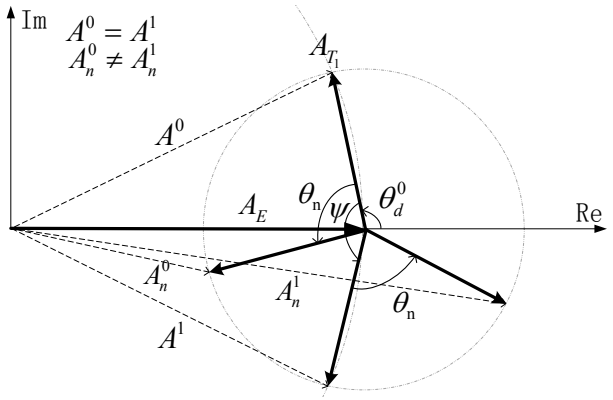

Fig. 9. Phasor diagrams of multi-phase backscattering and PSK modulation.

C. Combination of signals

In a straightforward implementation of the above method, a transmitting tag backscatters the same signal in successive intervals and the phase diversity ensures that one of these will be reliably detected by the receiving tag. This method also presents the opportunity to further improve performance by combining the backscattered signals received in the two intervals. Since the tag employs a purely analog circuit for envelope detection, one can develop a delay circuit to store the signal received in the first interval and then, combine it with the signal received in the second interval. With the envelope detector, one can form four amplitude differences: A_{d_1}, A_{d_2}, $A_{d_1} + A_{d_2}$ and $A_{d_1} - A_{d_2}$, where A_{d_1} and A_{d_2} are the amplitude differences in the first and second interval, respectively. The combination method can increase the differences of the amplitudes (almost double them), and therefore it can vastly improve the performance and communication

ranges of the BBTT system. Implementation of this scheme would require a protocol wherein individual bits of symbols of a tag are repeated rather than the whole message. This is because of the restriction on the amount of delay that can be built into the analog circuit. Because the demodulation is the same for the ASK and PSK modulations, this method can be applied to both of them. In our future work, we will explore designs for tags that utilize phase-diverse backscatter modulation along with the above described signal combination.

D. Discussion

Theoretically, the proposed methods can avoid the phase cancellation problem almost entirely. Our solution requires four impedances, small changes in the digital section of the tag, and minor changes in the protocol. The approach can be extended to include multiple impedances allowing for more phase diversity. As mentioned earlier, in one of our future works, we will be designing a protocol wherein two tags will first determine the best phase for backscattering during a handshaking period and then use that phase for communication. Having multiple possible impedances will be very beneficial in this approach.

Under a straightforward implementation (i.e., no signal combination, no special protocols) this proposed approach will increase the latency of the system. For most part, however, the applications of the BBTT system include backscattering of short messages. Therefore, the benefits of the multi-phase backscattering are much greater than the drawbacks.

We reiterate that the proposed solution cannot fully avoid the phase cancellation phenomenon using ASK modulation. Theoretically, when $\theta_d = \theta_c$ and $\theta_n = 2|\pi - \theta_d|$, θ_d changes from one cancellation phase $\theta_c \in (\frac{\pi}{2}, \pi]$ to another one, $2\pi - \theta_c$. Full cancellation can be avoided by using more impedances. Thus, we have a tradeoff between performance and latency.

V. Simulations Results

A. Simulations

Here we present simulation results that demonstrate the performance of the proposed approach. We use a very simple system with only two tags. Adding more tags to the system will not provide more insights about the studied problem, the models and the proposed solutions. If it is assumed that at any time only one tag is backscattering, phase cancellation can take place at any of the tags in its proximity.

We use a setting as shown in Fig. 1, where T_1 and the exciter are at fixed locations, and T_2 changes its location but stays in the plane defined by the locations of T_1, the exciter, and its initial location. More specifically, the position of T_1 is fixed at $(0, 0)$ and that of the exciter at $(0, 5)$ (thus, d_1 is equal to 5 m).

In the simulations, the power of the exciter was set at 13 dBm, and G_{T_1}, G_{T_2} and G_R in (15) were 2 dB and 6 dB, respectively. Also we set $k_0 = 0.15$, $k_1 = 0.8$, R = 50 Ω in (15) and θ_b due to Tag 1 for both states was equal to π. Because we do not consider the amplifier circuit and other hardware resistance, the presented values of the amplitudes are relative. Also we simulate the proposed method ideally, which means that we do not consider other random effects, such as noise and multipath. We only focus on the curves before and after using our solutions. The simulation results of the PSK modulation are very similar to those of the ASK modulation, and therefore we do not show them here.

B. Selection of θ_n

In (18), $k_0 + k_1$ is usually about 1 and $d_2 \approx d_1 >> d_3$. Since we use a UHF frequency, $\lambda \in [0.1, 1]$ m, and $\cos(\theta_c) = -\frac{(k_0+k_1)d_2\lambda G_{T1}}{8\pi d_1 d_3}$ is typically negative and very small. This means that θ_c is a little bit larger than $\frac{\pi}{2}$ or less than $\frac{3\pi}{2}$. From Figs. 4 and 8, when $\theta_d = \theta_c$, $\theta_d + \frac{\pi}{2}$ is close to π or 0, where we can obtain the largest amplitude differences between A^0 and A^1. So we fix θ_n to $\frac{\pi}{2}$.

C. Simulations in a two-dimensional space

First we show simulations in a two-dimensional space. In the experiment, Tag 2 only moves along the x axis starting at $(0, 0)$. We present the maximum amplitude difference between the two phases which reflect on the detection performance of the system. The results are shown in Fig. 10 for ASK modulation. The green line with downward-pointing triangle and the blue line with asterisk are the amplitude differences using one pair of impedances. When Tag 2 is in a position where $\theta_d = \theta_c$, the value of the green line is 0. While in this position, the value of the blue line is not 0. This means that Tag 2 does not receive the message during the first time period, but receives it during the second period.

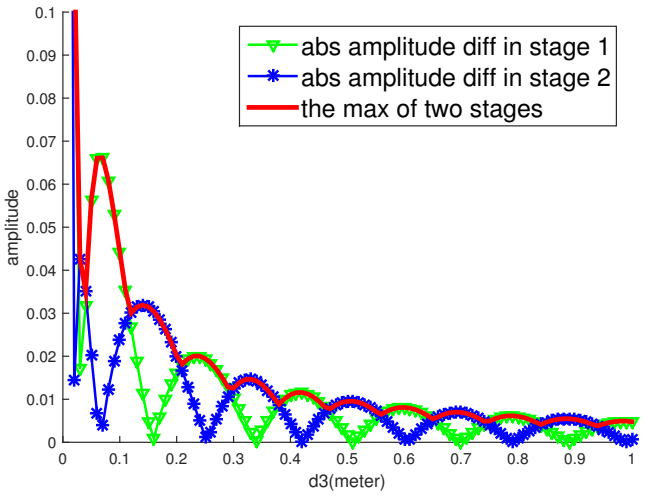

Fig. 10. The amplitude differences using the proposed method for ASK modulation in a two-dimensional space.

D. Simulations in a three-dimensional space

In these simulations, we use the same settings as in the simulations in the two-dimensional space, except that Tag 2 can be in any position whose x and y coordinates are within $[-2, 2]$ m. In the presentation of our results, we use a threshold value for detecting the signal. When the signal is detected in both phases, we use one symbol (and color), and similarly, different symbols (and colors) when the signal is detected only in the first or the second period, respectively.

The results are shown in Fig. 11. The red ($'\cdot'$) and blue points ($'*'$) are the positions where the tag can receive the signal in the first period, while the red and green ($'+'$) points are the positions where the tag successfully receives the signal in the second period. If we remove the green points, there are many positions where that tag cannot receive messages because of the phase cancellation problem. With the proposed method, the green points fill many new positions where the signal can be detected. However, there are still some locations where the signal is not detected, although the distances

between these positions suggest that detection should take place. This can be explained by noting the shape of the red line in Fig. 10. This line still has local dips, and the positions that are not filled correspond to some of them.

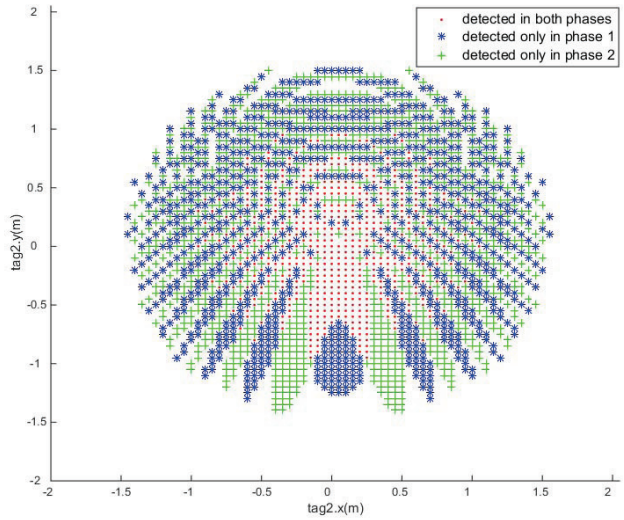

Fig. 11. The amplitude differences for ASK modulation in three-dimensional space using the proposed method.

VI. Experimental Results

In this section, we describe the experiments we performed to examine the phase cancellation phenomenon, verify our mathematical analysis and simulations, and evaluate our proposed solution.

A. Demonstration of the phase cancellation phenomenon

We use a setup as shown in Fig. 1 and consisting of two tags and one exciter. One of the tags is configured to be the transmitter, and it backscatters the signal it receives from the exciter. The other tag receives the backscatter and demodulates it using an envelope detector. The output of the envelope detector is observed on an oscilloscope. If the receiving tag is able to successfully demodulate the backscatter signal of the transmitting tag, the oscilloscope will show a square wave whose frequency is determined by the baseband frequency of the backscatter signal. As detailed in the previous sections, the amplitude of the observed square wave will not decrease monotonically as the distance between the tags increases, but will rather oscillate between peaks and nulls as a result of the superposition of the CW signal from the exciter and the backscatter signal from the tag. When perfect phase cancellation occurs, the amplitude of the square wave is zero.

For the exciter, we used a CW generator with frequency set to 915 MHz connected to a 6 dBiC antenna. Figure 12 shows the tag prototype that we used in this experiment. It consists of a printed dipole antenna connected to a backscatter modulator which includes an Agilent ADG 902 single pole double throw (SPDT) RF switch. The envelope detector used for demodulating the backscatter is built on a separate board using a Shottky diode doubler. The diode detector board is connected to one of the ports of the switch. This corresponds to state $'0'$ when the tag backscatters. A variable capacitance is connected to the other port of the switch and this corresponds to state $'1'$ of the backscattering tag. The switch control input of the transmitting (backscattering) tag is driven by a 100 kHz square wave signal generated using an MSP 430 microcontroller board. As a result, this tag generates modulated backscatter signal by reflecting the incident CW signal from the exciter.

At the receiving tag, the control signal of the switch (or backscatter modulator) is connected to ground, effectively connecting the tag antenna to the envelope detector without any backscattering. The demodulated baseband signal at the output of the envelope detector is connected to the oscilloscope. In Fig. 13, we show the experimental setup components of the system: one exciter, Tag 1 and Tag 2 (all circled). The prototype backscatter modulator is shown in Fig. 14.

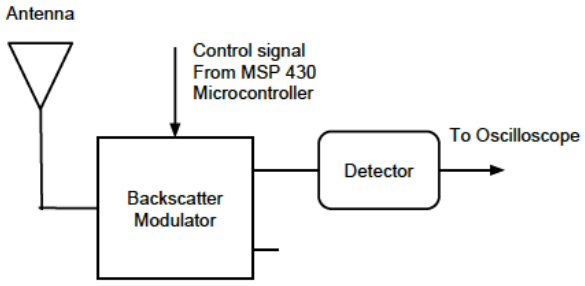

Fig. 12. The tag prototype.

Fig. 13. The experimental setup composed of one exciter and two tags.

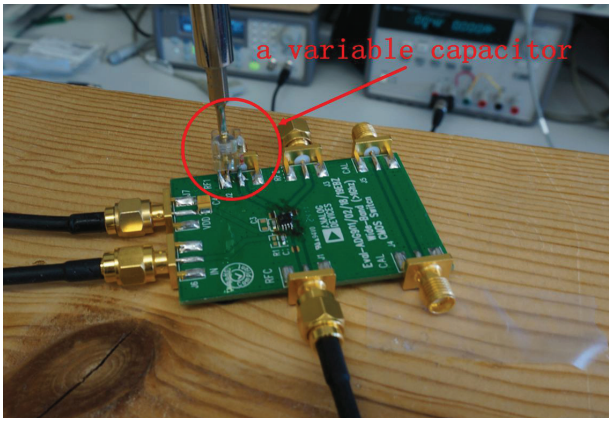

Fig. 14. A prototype backscatter modulator with a variable capacitor.

The CW generator and the MSP 430 output signal to the backscatter modulator were turned on, and the output of the envelope

detector at the receiving tag was observed on the oscilloscope. It was seen that when we moved the two tags apart in small increments the peak-to-peak amplitude of the observed square wave signal on the oscilloscope varied continuously between peaks and nulls with gradually decreasing peaks as the tag moved further away. This observation is in line with the simulations shown in Fig. 10. We note here that in these experiments our focus was specifically on the phase cancellation phenomenon rather than on the performance and sensitivity of the backscatter modulator or the envelope detector. Moreover, we have used prototype, non-optimized components in the setup of this experiment. Hence we do not measure the link performance extensively in terms of received amplitude versus distance, but rather verify the systematic occurrence of successive peaks and nulls confirming our mathematical analysis.

In another experiment, we connected a variable capacitor to the second throw of the backscatter modulator switch of the transmitting tag (the other throw still connected to the matched detector board). Using a network analyzer, the starting value of the variable capacitor was chosen to be sufficiently different from 50 Ω so as to generate a backscatter signal. We then placed the two tags close to each other (about 0.5 m apart) and turned on the CW generator and the backscatter modulator signal. Then observing the detector output at the receiving tag, we moved the tag away till we reached a position where the oscilloscope showed a straight line, i.e., there was complete phase cancellation. Then keeping the positions of all devices the same, we manually varied the capacitance connected to the backscatter modulator while observing the detected backscatter. The experimental results are shown in Figs. 15, 16, and 17. We can clearly see that when the variable capacitor changes the phase of the backscatter, the amplitude difference becomes much larger than in Fig. 15. In other words, by introducing phase diversity in the backscattering, the two tags are able to overcome the null and communicate with each other. This experiment demonstrates that the multi-phase backscattering approach can be successfully used to alleviate the phase cancellation problem.

We would like to point out that the phase cancellation problem itself can also be demonstrated by using a standard RFID reader as an exciter, a standard RFID tag as the transmitting tag and a similar (envelope detector/oscilloscope) setup for the receiving tag. We have observed phase cancellation during some of our prior work [10].

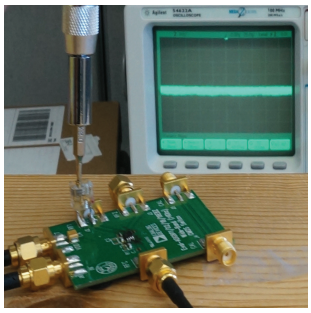

Fig. 15. Phase cancellation. The amplitude difference between the states is about 0.

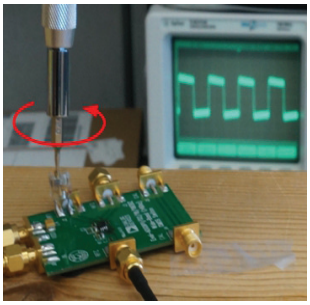

Fig. 16. The amplitude diference between the two states increases when the value of the variable capacitor changes.

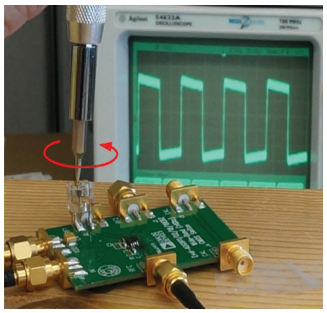

Fig. 17. The amplitude difference between the two states when the phase do to the capacitor changes is about $\pi/2$.

B. Implementation of proposed solution

The above two experiments clearly show the presence of phase cancellation in BBTT systems and that our proposed multi-phase backscattering approach can overcome it. In order to evaluate this approach, we built a prototype backscattering tag wherein an SP4T RF switch was used as the backscatter modulator rather than the SPDT switch used in the earlier experiments. This is an implementation of the backscatter modulator shown in Fig. 7. One of the throws of the switch is connected to a matched envelope detector. The second one is left open and the third one is connected to a capacitor that introduces a close to $\pi/2$ phase shift in the backscattered signal. Two outputs of an MSP 430 microcontroller were used to drive the backscatter modulator. The device was programmed to backscatter a 10 kHz signal for 25 ms by switching between throws 1 and 2, and then backscatter the same signal with a close to $\pi/2$ phase for the next 25 ms by switching between throws 1 and 3.

At the receiving tag, the output of the envelope detector was sampled and recorded using the ADS660EVM-PDK analog-to-digital converter evaluation module from Texas Instruments. The distance between the two tags was increased in increments of 5 cm and 100 ms of received data was sampled and stored. As mentioned earlier, the backscattering tag uses our multi-phase backscattering scheme and repeats the same data at two different phases. Fig. 18 shows the measured peak-to-peak amplitude of the received signal at the output of the envelope detector with increasing distance between the two tags. It can be seen that these results are in agreement with Fig. 11 with respect to the frequency and pattern of the nulls. Furthermore, we see that when one of the phases results in a null, the two tags can still communicate at the other phase. This validates our proposed approach circumvent the cancellation.

With these experiments, we have validated that our solution circumvents the phase cancellation problem.

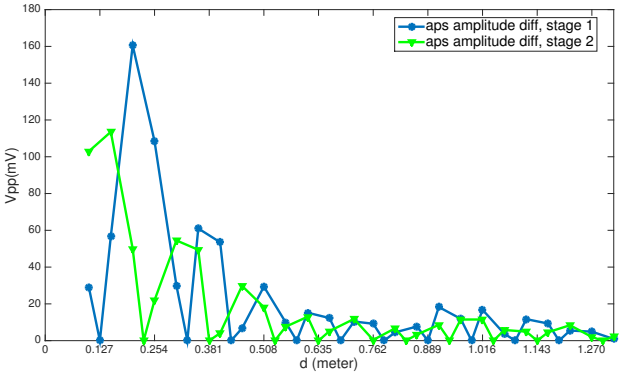

Fig. 18. Peak-to-peak amplitude of backscatter signal at the receiving tag for the two backscattering phases.

VII. Conclusion

In this paper, we described the phase cancellation problem of backscatter-based tag-to-tag communication systems. In these sys-

tems, a tag receives the superposition of a CW and backscatter signals which have the same frequency but different phases. The combination of these two signals may cause that a tag cannot discriminate between the signals corresponding to states $'1'$ and $'0'$. We addressed and analyzed the problem for both ASK and PSK modulations. We presented several solutions and proposed a multi-phase backscattering method. According to the method, a tag sends a message twice using different pair of impedances. Our simulations show that for ASK and PSK modulations phase cancellation can greatly be reduced. We have verified our simulations in lab experiments.

Acknowledgment: We thank Jianhui Jian and Jihoon Ryoo for performing the experiments whose results are presented in Fig. 18.

REFERENCES

[1] D. M. Dobkin, *The RF in RFID: UHF RFID in Practice*. Newnes, 2012.

[2] D.-Y. Kim, H.-G. Yoon, B.-J. Jang, and J.-G. Yook, "Effects of reader-to-reader interference on the UHF RFID interrogation range," *Industrial Electronics, IEEE Transactions on*, vol. 56, no. 7, pp. 2337–2346, July 2009.

[3] V. Liu, A. Parks, V. Talla, S. Gollakota, D. Wetherall, and J. R. Smith, "Ambient backscatter: wireless communication out of thin air," in *ACM SIGCOMM Computer Communication Review*, vol. 43, no. 4. ACM, 2013, pp. 39–50.

[4] B. Kellogg, A. Parks, S. Gollakota, J. R. Smith, and D. Wetherall, "Wi-Fi backscatter: Internet connectivity for RF-powered devices," in *Proceedings of the 2014 ACM conference on SIGCOMM*. ACM, 2014, pp. 607–618.

[5] D. Bandyopadhyay and J. Sen, "Internet of Things: Applications and challenges in technology and standardization," *Wireless Personal Communications*, vol. 58, no. 1, pp. 49–69, 2011.

[6] M. Bolic, M. Rostamian, and P. M. Djurić, "Proximity detection with RFID: A step toward the internet of things," *IEEE Pervasive Computing*, no. 2, pp. 70–76, 2015.

[7] P. V. Nikitin, S. Ramamurthy, R. Martinez, and K. Rao, "Passive tag-to-tag communication," in *RFID (RFID), 2012 IEEE International Conference on*. IEEE, 2012, pp. 177–184.

[8] G. Marrocco and S. Caizzone, "Electromagnetic models for passive tag-to-tag communications," *IEEE Transactions on Antennas and Propagation*, vol. 60, no. 11, pp. 5381–5389, 2012.

[9] P. Djurić and A. Athalye, "RFID system and method for localizing and tracking a moving object with an RFID tag," Oct. 12 2010, uS Patent 7,812,719. [Online]. Available: https://www.google.com/patents/US7812719

[10] A. Athalye, V. Savić, M. Bolić, and P. Djurić, "Novel semi-passive RFID system for indoor localization," *Sensors Journal, IEEE*, vol. 13, no. 2, pp. 528–537, Feb 2013.

[11] K. Kurokawa, "Power waves and the scattering matrix," *IEEE Transactions on Microwave Theory and Techniques*, vol. 13, no. 2, pp. 194–202, 1965.

[12] P. V. Nikitin, K. S. Rao, S. F. Lam, V. Pillai, R. Martinez, and H. Heinrich, "Power reflection coefficient analysis for complex impedances in RFID tag design," *IEEE Transactions on Microwave Theory and Techniques*, vol. 53, no. 9, pp. 2721–2725, 2005.

[13] J. Wang and M. Bolić, "Exploiting dual-antenna diversity for phase cancellation in augmented RFID system," in *Smart Communications in Network Technologies (SaCoNeT), 2014 International Conference on*. IEEE, 2014, pp. 1–6.

[14] J. Wang and M. Bolic, "Reducing phase cancellation effect with ASK-PSK modulated stamp in augmented UHF RFID indoor localization system," *Procedia Computer Science*, vol. 56, pp. 465–470, 2015.

[15] S. J. Thomas, E. Wheeler, J. Teizer, and M. S. Reynolds, "Quadrature amplitude modulated backscatter in passive and semipassive uhf rfid systems," *Microwave Theory and Techniques, IEEE Transactions on*, vol. 60, no. 4, pp. 1175–1182, 2012.

[16] C. Boyer and S. Roy, "Coded QAM backscatter modulation for RFID," *Communications, IEEE Transactions on*, vol. 60, no. 7, pp. 1925–1934, 2012.

[17] S. Thomas and M. S. Reynolds, "QAM backscatter for passive UHF RFID tags," in *RFID, 2010 IEEE International Conference on*. IEEE, 2010, pp. 210–214.